Human Molecular Genetics, 2015, Vol. 24, No. 4 **939–953**
doi:10.1093/hmg/ddu506
Advance Access published on October 14, 2014

Deletion of OTX2 in neural ectoderm delays anterior pituitary development

Amanda H. Mortensen[1], Vanessa Schade[1], Thomas Lamonerie[2] and Sally A. Camper[1,*]

[1]Department of Human Genetics, University of Michigan, Ann Arbor, MI 48109-5618, USA and [2]Institut de Biologie Valrose, University of Nice Sophia Antipolis, CNRS UMR7277, Inserm U1091, Nice 06108, France

Received June 17, 2014; Revised August 19, 2014; Accepted September 29, 2014

OTX2 is a homeodomain transcription factor that is necessary for normal head development in mouse and man. Heterozygosity for loss-of-function alleles causes an incompletely penetrant, haploinsufficiency disorder. Affected individuals exhibit a spectrum of features that range from developmental defects in eye and/or pituitary development to acephaly. To investigate the mechanism underlying the pituitary defects, we used different cre lines to inactivate *Otx2* in early head development and in the prospective anterior and posterior lobes. Mice homozygous for *Otx2* deficiency in early head development and pituitary oral ectoderm exhibit craniofacial defects and pituitary gland dysmorphology, but normal pituitary cell specification. The morphological defects mimic those observed in humans and mice with *OTX2* heterozygous mutations. Mice homozygous for *Otx2* deficiency in the pituitary neural ectoderm exhibited altered patterning of gene expression and ablation of FGF signaling. The posterior pituitary lobe and stalk, which normally arise from neural ectoderm, were extremely hypoplastic. *Otx2* expression was intact in Rathke's pouch, the precursor to the anterior lobe, but the anterior lobe was hypoplastic. The lack of FGF signaling from the neural ectoderm was sufficient to impair anterior lobe growth, but not the differentiation of hormone-producing cells. This study demonstrates that *Otx2* expression in the neural ectoderm is important intrinsically for the development of the posterior lobe and pituitary stalk, and it has significant extrinsic effects on anterior pituitary growth. *Otx2* expression early in head development is important for establishing normal craniofacial features including development of the brain, eyes and pituitary gland.

INTRODUCTION

Patients heterozygous for mutations in the transcription factor OTX2 exhibit a spectrum of phenotypes that can include severe ocular defects, central nervous system abnormalities, developmental delay, endocrine deficiencies, and/or structural and functional abnormalities of the pituitary gland (1–6). The pituitary gland defects, if present, are also variable and can include isolated growth hormone deficiency (IGHD), combined pituitary hormone deficiency (CPHD), hypogonadotropic hypogonadism, anterior pituitary hypoplasia, ectopic neurohypophysis (posterior pituitary lobe) and disrupted pituitary stalk [reviewed (7)]. The majority of the reported mutations are nonsense mutations or frameshifts that result in truncated proteins (1,3–6,8). Functional studies demonstrate that truncation of the OTX2 protein leads to reduced transactivation activity, although some mutations may act in a dominant-negative manner (2,3,5). No clear genotype–phenotype correlation is associated with these mutations, and phenotypic variability occurs even among individuals with the same mutation (2,5,8). Furthermore, OTX2 mutations that have been examined in families all exhibit incomplete penetrance, which may be due to the influence of modifying effects of other genes or epigenetic events (9). In one typical example, a patient heterozygous for an OTX2 mutation presented with short stature, IGHD, pituitary hypoplasia, ectopic posterior pituitary gland and anophthalmia. The father carried the same mutation, and although he had short stature (<5th percentile), he did not have any ocular or pituitary defects (10).

Studies in mice support the idea that the incomplete penetrance of *OTX2* loss-of-function mutations is caused by modifier genes that enhance or suppress the phenotype. Homozygous deletion of *Otx2* consistently causes embryonic lethality in mice because they lack the rostral neural ectoderm, from which the

*To whom correspondence should be addressed at: Department of Human Genetics, University of Michigan, 4909 Buhl Building, 1241 Catherine Street, Ann Arbor, MI 48109-5618, USA. Tel: +1 7347630682; Fax: +1 7347633784; Email: scamper@umich.edu

forebrain, midbrain and rostral hindbrain arise (11). Heterozygous mutant mice have a variable phenotype that resembles aspects of the *OTX2* features in human patients. The phenotypic range spans from unaffected, to craniofacial malformations affecting the eyes (anophthalmia and microphthalmia), jaw (agnathia and micrognathia) and nose, and, finally, to severe developmental defects of the head (acephaly and holoprosencephaly) (12). The pituitary phenotypes extend from deformities of the posterior pituitary lobe and dysmorphology of the anterior lobe (adenohypophysis) to pituitary aplasia. The genetic background of the mice affects the severity and frequency of all of the phenotypes, C57BL/6 enhances the phenotype of heterozygous mutants and CBA suppresses it. Genetic mapping revealed the presence of two interacting loci that underlie this variation, but the genes are unknown (13).

OTX2 has been proposed to influence pituitary development by regulating expression of two transcription factors that are important for anterior pituitary development: HESX1 and POU1F1 (4,5,10). For a review of pituitary organogenesis, see Davis *et al*. (2009) (14). If OTX2 was a direct, master regulator of either of these genes, there would be overlap in the expression patterns. The temporal and spatial expression of these three transcription factors and their loss-of-function phenotypes suggest a different and complex underlying mechanism, however.

The correspondence between *Otx2* and *Hesx1* expression in early embryogenesis supports the idea that OTX2 regulates *Hesx1* in developing anterior structures (15,16). Both genes are expressed prior to implantation, and at gastrulation, their expression becomes localized in the anterior visceral endoderm (AVE) and later in the neural ectoderm, respectively (17–22). In addition, both genes are expressed in the forebrain. There are many similarities in loss-of-function phenotypes of *Hesx1* and *Otx2* mutants, including development of the head, eyes, brain and pituitary gland (23,24). This is consistent with the idea that *Otx2* regulates *Hesx1* in early head development.

During pituitary development, the expression of *Otx2* is broader than *Hesx1*. *Otx2* is expressed at e10.5 in the ventral diencephalon, which will become the pituitary stalk and posterior lobe, and it persists there through e16.5. *Hesx1* is not expressed in the ventral diencephalon or posterior lobe. Both *Otx2* and *Hesx1* are expressed modestly in Rathke's pouch, which eventually develops into the intermediate and anterior pituitary lobes. *Otx2* expression is silenced by e12.5, and *Hesx1* is by e14.5 (19,22,25). Thus, it is possible that *Otx2* regulates *Hesx1* in the oral ectoderm that produces the pouch, and in early head development, but not in the neural ectoderm that becomes the posterior lobe.

There is no overlap between *Otx2* and *Pou1f1* expression in the pituitary primordium or anterior lobe. *Pou1f1* is expressed almost exclusively in the developing anterior lobe, and transcripts are not detectable until e14.5, well after *Otx2* and *Hesx1* expression is silenced (26). In addition, *Pou1f1* mutations only affect the differentiation of three pituitary hormone-producing cell types leading to a triad of pituitary hormone deficiencies: thyrotropin (TSH), growth hormone (GH) and prolactin (27–31). If there is a role for *Otx2* in Rathke's pouch, it does not involve direct regulation of *Pou1f1*.

We hypothesize that OTX2 promotes anterior pituitary development by activating target genes in the neural ectoderm. To test this idea, we generated conditional deletions of *Otx2* in the neural ectoderm and in the oral ectoderm. Our data with the conditional oral ectoderm knockouts suggest that *Otx2* plays a minor role, if any, in the organogenesis of Rathke's pouch. We discovered that *Otx2* expression in the neural ectoderm, however, is necessary for normal development of the infundibulum or pituitary stalk, and for initial induction of FGF signaling in the ventral diencephalon. FGF signaling is known to have a crucial role in anterior pituitary gland growth and development (32). Thus, *Otx2* deficiency in the neural ectoderm is sufficient to delay normal growth and development of the anterior pituitary gland.

RESULTS

Conditional *Otx2* oral ectoderm knock out

We sought to remove *Otx2* in the prospective anterior lobe of the pituitary gland using the *Foxg1-cre* mouse line (33). *Foxg1-cre* expression is reported to be detectable in every cell in the oral ectoderm that gives rise to the anterior and intermediate lobes of the pituitary, before the closure of Rahtke's pouch at e9.5. There is no expression of *Foxg1-cre* in the ventral diencephalon (34). We mated $Otx2^{FX/+}$; *Foxg1-cre* mice to $Otx2^{FX/FX}$ mice to generate $Otx2^{FX/FX}$; *Foxg1-cre* mice which were designated as mutants ($Otx2^{FX}$;*Foxg1-cre*) and $Otx2^{FX/FX}$ and $Otx2^{FX/+}$ mice were designated as controls.

$Otx2^{FX}$;*Foxg1-cre* embryos collected at e14.5 had obvious craniofacial deformities that mimic those found in *OTX2* heterozygote humans and mice (12,35,36). At e12.5 and e14.5, the defects in $Otx2^{FX}$;*Foxg1-cre* mutants include microphthalmia or anophthalmia, facial defects and/or excencephaly ($n = 7$) (Fig. 1A and C). This indicates inactivation of *Otx2* early during head development, and a lack of anterior pituitary specificity. The pituitary glands of the mutants exhibited a variety of phenotypes that include dysmorphology, protrusion through the palate, misplacement of a hypoplastic pituitary in the head or a relatively normal looking pituitary ($n = 6$). All the $Otx2^{FX}$;*Foxg1-cre* pituitaries express the pituitary transcription factors PITX1 at e14.5 and *Hesx1* at e11.5. Immunostaining of the mutant anterior pituitaries revealed normal expression of the signature transcription factors POU1F1 (somatotropes, lactotropes and thyrotropes), TPIT (corticotropes) and the hormone subunit αGSU, which marks gonadotropes and thyrotropes, at e14.5 (Fig. 1B). These data suggest that the morphological defects characteristic of the $Otx2^{FX}$;*Foxg1-cre* pituitaries are due to loss of OTX2 during early head development, whereas loss of OTX2 expression in Rathke's pouch does not affect cell specification.

We used a different *cre* line, *Pitx2-cre*, to conditionally delete *Otx2* in the oral ectoderm that gives rise to the pituitary gland. The *cre* cassette is inserted into exon 5 of the *Pitx2* gene (37). The $Otx2^{FX/FX}$ (38) mouse was crossed with a *cre* reporter strain consisting of a floxed stop sequence, which upon *cre*-mediated excision permits lacZ expression ($R26R^{FX/FX}$) (39). The $Otx2^{FX/FX}$; $R26R^{FX/FX}$ offspring were mated to $Otx2^{FX/+}$; *Pitx2-cre*$^{+/-}$ mice. Mice with genotype $Otx2^{FX/FX}$; $R26R^{FX/+}$; *Pitx2-cre*$^{+/-}$ are designated as mutants ($Otx2^{FX}$; *Pitx2-cre*) and $Otx2^{FX/+}$; $R26R^{FX/+}$ mice serve as normal controls. We assessed the efficiency and penetrance of *cre*-mediated recombination using X-gal staining of frozen sections from e11.5 embryos (Supplementary Material, Fig. S1A). The mutant

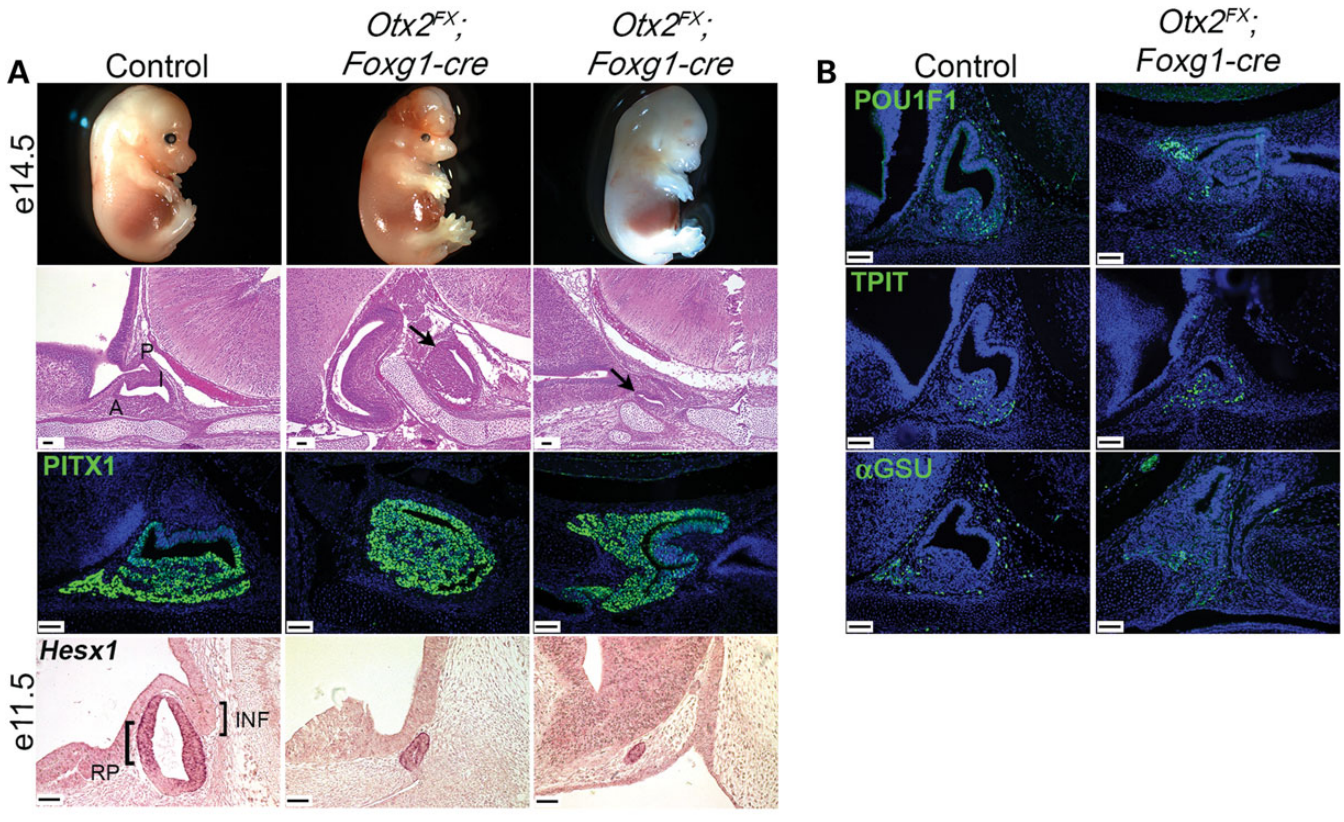

C

Description of External Defects

Otx2^{FX};*Foxg1-cre* mutant mouse	Age	Eye Defect	No Eyes	Facial Defect	Excencephaly	Growth Defect
1	e12.5	x			x	
2	e12.5	x		x		
3	e12.5		x	x	x	x
4	e14.5	x		x		
5	e14.5		x			
6	e14.5	x		x	x	
7	e14.5	x		x		
Total		100%		71%	43%	14%

Figure 1. (**A**–**C**) *Otx2*^{FX}*;Foxg1-cre*-mutant embryos have craniofacial defects and dysmorphic pituitary glands. (A) At e14.5, *Otx2*^{FX}*;Foxg1-cre*-mutant embryos exhibit craniofacial (top middle panel) and ocular defects (top right panel). Hematoxylin and eosin staining of e14.5 sagittal sections of *Otx2*^{FX}*;Foxg1-cre* mutants reveal dysmorphic pituitary glands (arrow in middle panel and right panels). A—anterior pituitary lobe, I—intermediate pituitary lobe, P—posterior pituitary lobe. Photos were taken at. Scale bar: 100 μm. Immunostaining for PITX1 reveals which tissues are pituitary specific in the *OTX2*^{FX}*;Foxg1-cre* mutants at e14.5. The photos in the third panel were taken at ×200. Scale bar: 50 μm. *In situ* hybridization for *Hesx1* shows normal expression in smaller *Otx2*^{FX}*;Foxg1-cre* mutant pituitaries at e11.5. RP—Rathke's Pouch, INF—infundibulum. The photos in the bottom panel were taken at. Scale bar: 50 μm. (B). *Otx2*^{FX}*;Foxg1-cre* mutants express POU1F1, TPIT and αGSU at e14.5 when compared with control pituitaries. Expression was variable and dependent on the growth of the mutant anterior lobe. Photos were taken at. Scale bar 50 μm. (C) Chart quantifying external defects observed in *Otx2*^{FX}*;Foxg1-cre*-mutant embryos at e12.5 and e14.5 ($N = 7$).

embryos consistently had blue X-gal staining in approximately two-thirds of the cells in Rathke's pouch, and no cells were stained in the ventral diencephalon ($n = 3$). There is no evidence of nonspecific X-gal staining in normal embryos ($n = 3$). Hematoxylin and eosin staining of sections from e14.5 mutant embryos revealed no morphological difference between the *Otx2*^{FX}*;Pitx2-cre* mutants and controls (Supplementary Material, Fig. S1B). Furthermore, the mutant pituitaries exhibited normal cell specification because e14.5 mutant embryos had normal immunostaining for αGSU and POU1F1 (Supplementary Material, Fig. S1B), and the P10 neonates had normal immunostaining for GH, TSHβ, ACTH and LHβ (data not shown). This is consistent with the idea that the pituitary defects in the *Otx2*^{FX}*;Foxg1-cre* mice result from deletion of *Otx2* in early head development, not Rathke's pouch.

Conditional *Otx2* neural ectoderm knock out

To generate conditional *Otx2* neural ectoderm knockout mice, we mated the *Otx2*$^{FX/FX}$ (38) mouse to the *Nkx2.1-cre* driver strain in which the *cre* cassette is inserted at the *Nkx2.1* locus (40). The *Otx2*$^{FX/FX}$*; R26R*$^{FX/FX}$ offspring were then mated

to $Otx2^{FX/+}$; $Nkx2.1\text{-}cre^{+/-}$ mice. Mice with the genotype $Otx2^{FX/FX}$; $R26R^{FX/+}$; $Nkx2.1\text{-}cre^{+/-}$ are designated as mutants ($Otx2^{FX}$;*Nkx2.1-cre*), and $Otx2^{FX/+}$; $R26R^{FX/FX}$ mice serve as normal controls. We assessed the efficiency and penetrance of *cre*-mediated recombination using X-gal staining of frozen sections from e11.5 $Otx2^{FX}$;*Nkx2.1-cre* mutant and control embryos (Fig. 2A). The mutant embryos consistently had blue X-gal staining throughout the ventral diencephalon, but staining in Rathke's pouch was minimal: only 1/7 embryos had X-gal stained cells in Rathke's pouch. There is no evidence of other nonspecific X-gal staining in $Otx2^{FX}$;*Nkx2.1-cre* embryos ($n = 7$). To verify that *Otx2* was effectively knocked out in the ventral diencephalon, we used immunohistochemistry to detect the OTX2 protein at e11.5, e12.5 and e14.5. Almost no OTX2 protein was detected in the ventral diencephalon in the $Otx2^{FX}$;*Nkx2.1-cre* mutants at either time (Fig. 2B) ($N = 3$ for e11.5, $N = 3$ for e12.5 and $N = 5$ for e14.5). OTX2 immunostaining in Rathke's pouch of the mutant is indistinguishable from the wild type, affirming that this transgenic knockout strategy effectively and specifically removed OTX2 expression from the ventral diencephalon.

Neural ectoderm knockout of *Otx2* results in poor posterior lobe formation and a smaller anterior pituitary gland

To assess the effects of neural-ectoderm-specific deletion of *Otx2*, we examined the morphology of $Otx2^{FX}$;*Nkx2.1-cre* mutant pituitaries using hematoxylin and eosin staining of sections from embryos collected at e10.5, e12.5, e14.5 and e16.5 ($n = 3$ or greater for each time point). There was no evidence of invagination of the ventral diencephalon, which is necessary for forming the infundibulum and posterior lobe of the pituitary gland. Indeed, at e14.5 and e16.5, there appears to be no posterior lobe present in sagittal sections (Fig. 3A). There were no distinguishable abnormalities in Rathke's pouch development in $Otx2^{FX}$;*Nkx2.1-cre* mutants at e10.5, when the ventral diencephalon begins to invaginate and the pouch is induced. While *Otx2* knockout in the neural ectoderm did not affect the separation of Rathke's pouch from the oral ectoderm, the mutant pouch is obviously hypoplastic at e14.5. The genetic background of the $Otx2^{FX}$; *Nkx2.1cre* is mixed, consisting of C57BL/6J and 129/SV, but there is no obvious phenotypic variability in the pituitaries of these animals.

We investigated further by staining serial coronal pituitary sections of e14.5 $Otx2^{FX}$;*Nkx2.1-cre* mutants and normal littermates with hematoxylin and eosin. A nubbin of tissue resembling the posterior lobe was noted at 100% penetrance and in at least three sections per animal. (Fig. 3B). To determine whether this tissue was specified as posterior lobe, we carried out immunostaining for the co-repressor TLE4 (transducin-like enhancer of split), which is normally concentrated in the developing posterior lobe at e14.5 (41). The nubbin of tissue in the $Otx2^{FX}$;*Nkx2.1-cre* mutant animals expressed TLE4, indicating commitment to the posterior lobe fate (Fig. 3, $n = 3$ per genotype). We also examined OTX2 immunostaining in $Otx2^{FX}$;*Nkx2.1-cre* mutants at e14.5 and found minimal OTX2 staining in the posterior lobe tissue, indicating efficient, specific elimination of OTX2 (Fig. 3B, $n = 4$). Occasionally, a few cells with OTX2 expression were detected in posterior pituitary tissue. *In situ* hybridization with the *Otx2 in situ* probe mimicked the results seen with the OTX2 antibody (Fig. 3B, $n = 3$). These data indicate that the nubbin of posterior pituitary tissue present

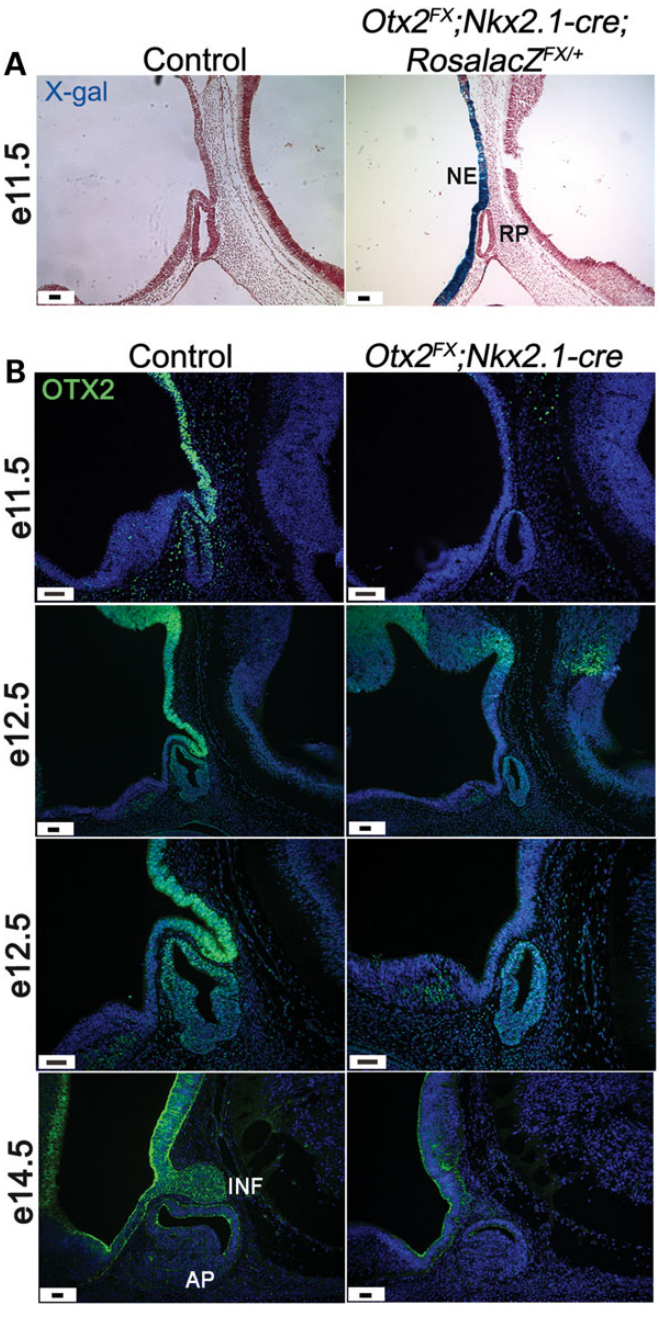

Figure 2. (**A** and **B**) *Nkx2.1-cre* activity is specific to the ventral diencephalon and is effective at removing OTX2 expression. (A) Sagittal frozen sections of e11.5 control and $Otx2^{FX}$;*Nkx2.1cre;*$RosalacZ^{FX/+}$ mutant embryos were examined with Xgal staining to assess *cre* activity and effective recombination. NE—neural ectoderm, RP—Rathke's Pouch. Photos were taken at. Scale bar: 100 μm. (B) Immunohistochemistry of OTX2 protein on sagittal sections at e11.5, e12.5 and e14.5 reveal that OTX2 expression is absent from the ventral diencephalon in the $Otx2^{FX}$;*Nkx2.1-cre* mutant pituitaries. INF—infundibulum, AP—anterior pituitary. The photos in the top and bottom panels were taken at. Scale bar: 100 μm. The photos in the middle panel were taken at. Scale bar 50 μm.

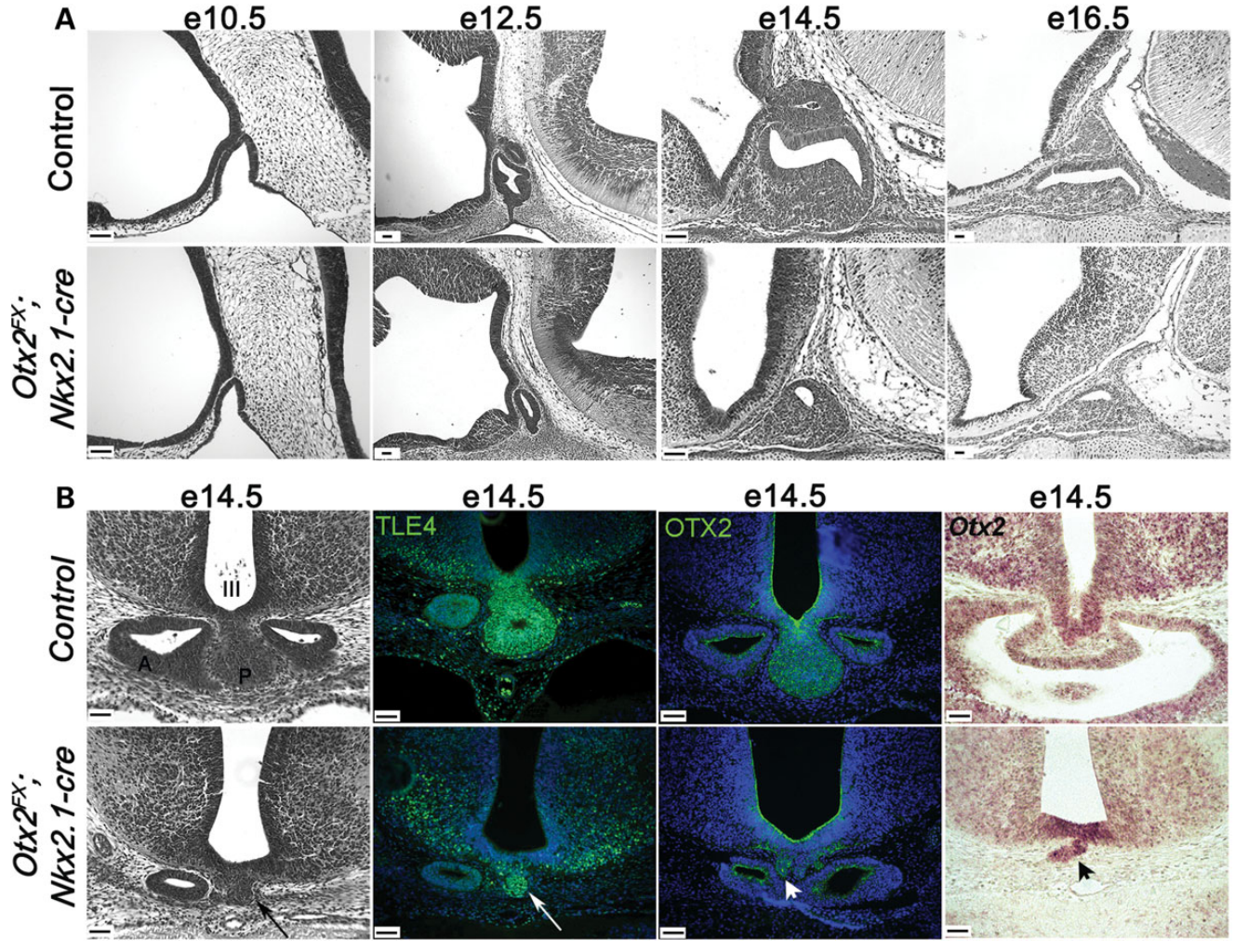

Figure 3. (**A** and **B**) Loss of OTX2 in the ventral diencephalon results in a smaller, dysmorphic pituitary gland. (A) e10.5, e12.5, e14.5 and e16.5 sagittal pituitary sections were stained using hematoxylin and eosin. At e10.5, there is no difference between $Otx2^{FX/+}$ wild-type (top panel) and $Otx2^{FX}$;*Nkx2.1-cre* mutants (bottom panel). At e12.5 through e16.5, there is a lack of invagination of the infundibulum and a smaller anterior lobe in the mutants compared with the wild types. The e10.5 and e14.5 photos were taken at ×200. Scale bar: 50 μm. The e12.5 and e16.5 photos were taken at ×100. Scale bar: 100 μm. (B) e14.5 coronal pituitary sections were stained using hematoxylin and eosin, revealing a slight invagination of ventral diencephalon in the mutants (black arrow). TLE4 immunostaining at e14.5 identifies the reduced evagination of the posterior lobe in the $Otx2^{FX}$;*Nkx2.1-cre* mutants (white arrow). OTX2 immunostaining in control and $Otx2^{FX}$;*Nkx2.1-cre*-mutant animals at e14.5 reveals some OTX2 protein in the small mutant posterior lobe (white arrowhead.) *In situ* hybridization for *Otx2* in the control and $Otx2^{FX}$;*Nkx2.1-cre* mutants reveals some transcripts in the small, mutant posterior lobe (black arrow head). III—third ventricle, A—anterior lobe, P—posterior lobe. Photos were taken at. Scale bar: 50 μm.

in the mutants is unlikely to have arisen from cells in the ventral diencephalon that escaped *Otx2* deletion.

At postnatal day 2 (P2), both the posterior and anterior lobes of $Otx2^{FX}$;*Nkx2.1-cre* mutants are significantly smaller than normal (Fig. 4A). There were significantly fewer sections with pituitary tissue in embryos collected at either e14.5 or P2 (Fig. 4B). The overall reduction in pituitary tissue was comparable at e14.5 and P2, 41 and 40, respectively. The size reduction was similar in the P2 anterior and posterior lobes: 52 and 38%, respectively (Fig. 4C). Surprisingly, improved mutant pituitary growth is evident at P10 (Fig. 4A). There were significantly fewer sections of $Otx2^{FX}$;*Nkx2.1 cre* mutant pituitary tissue at P10, but the size was only reduced by 22% (Fig. 4B). These results suggest that the primary effect of knocking OTX2 out of the ventral diencephalon is a delay in posterior lobe formation, and secondary to that, the size of Rathke's pouch is decreased.

FGF signaling is disrupted in the $Otx2^{FX}$; *Nkx2.1-cre* knockout pituitary

We tested the hypothesis that *Otx2* expression in the neural ectoderm is necessary for FGF signaling, which in turn is required for stimulating anterior pituitary development. FGF signaling normally emanates from the ventral diencephalon from e9.0 to e14.5 (16), and deficiency of FGF10 (32) or FGFr2b (42) is sufficient to cause failed anterior pituitary development. We examined FGF signaling in $Otx2^{FX}$; *Nkx2.1-cre* mutants by performing *in situ* hybridization for *Fgf10* at e12.5. We found that *Fgf10* expression is greatly decreased in the $Otx2^{FX}$; *Nkx2.1-cre* mutant ventral diencephalon compared with normal controls (Fig. 5A). Multiple FGFs are expressed in the ventral diencephalon, and they all should increase the phosphorylation of ERK (pERK). We carried out immunostaining for pERK in sections

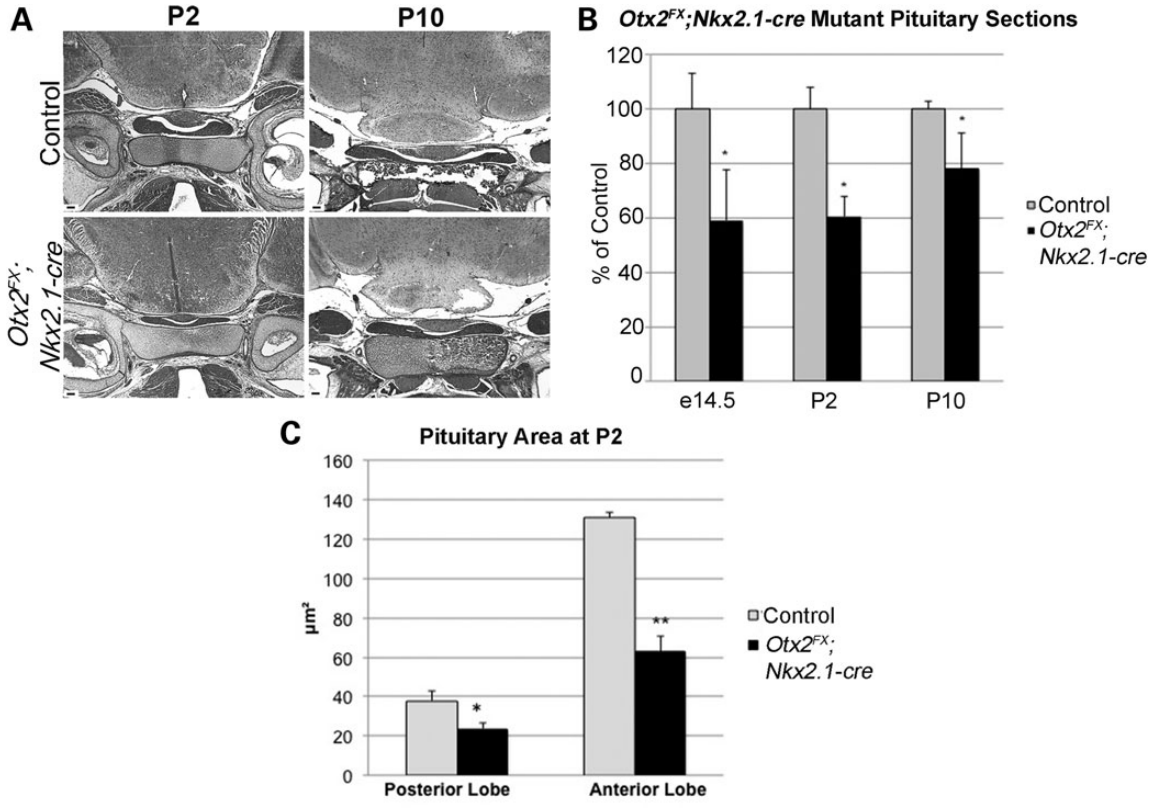

Figure 4. (**A** and **B**) Delayed invagination of the posterior lobe in *Otx2^{FX};Nkx2.1-cre* mutants. (A) Coronal sections at P2 and P10 were hematoxylin and eosin stained. Photos were taken at. Scale bar: 100 μm. (B) Relative pituitary size was measured at e14.5, P2 and P10. Three control and three mutant animals were sectioned and mounted two sections per slide. Sections containing pituitary gland tissue were counted and averaged, and percentages were calculated. *P*-values for control (gray bars) compared with mutants (black bars) were determined using the average number of sections and the Student's *T*-test for each age group: *P*-value < 0.05 (*). (**C**) ImageJ IJ 1.46r software from the NIH was used to measure the posterior and anterior lobes of three control and three mutants with four sections per sample. The Student's *T*-test was used to calculate *P*-values for controls compared with *Nkx2.1cre$^{+/-}$* mutants for each age group: *P*-value < 0.05 (*) for posterior lobe; *P*-value < 0.01 (**) for anterior lobe.

from e11.5 embryos. There is an obvious decrease in pERK immunostaining in the ventral diencephalon of the *Otx2^{FX}; Nkx2.1-cre* mutant relative to normal controls (Fig. 5A), which is consistent with an overall deficiency in FGF signaling. These results suggest that the delay in posterior lobe formation causes decreased FGF signaling, which secondarily decreases the growth of Rathke's pouch.

Disrupting a single signaling pathway can impact the expression of other signaling pathways and affect patterning of the ventral diencephalon. Loss of expression of genes, such as *Noggin*, *Tcf7l2* and *Wnt5a*, in the dorsal aspect of the ventral diencephalon where FGF is normally expressed, can permit expansion of the expression domains of genes typically restricted to the rostral aspect (43–45). We examined the expression domains of the transcription factor *Six6* (Fig. 5B) and the signaling by sonic hedgehog (SHH, Fig. 5B) by *in situ* hybridization and immunostaining, respectively. The expression pattern of both genes appeared to obey the molecular boundary between the dorsal-caudal and rostral-ventral areas of the ventral diencephalon. *Nkx2.1* is typically expressed throughout the ventral diencephalon at e11.5, and the *Otx2^{FX};Nkx2.1-cre* mutants had no disruption in expression detected by *in situ* hybridization (Fig. 5B). TLE4 is normally expressed in two domains of the ventral diencephalon: in the dorsal-caudal area ending at the rostral, ventral aspect of the posterior lobe, and in the area rostral and ventral to Rathke's pouch, but only on the inner area of the neural ectoderm in this region. The outer area of the neural ectoderm, at the ventricular zone, is devoid of Tle4 expression. Immunohistochemistry for TLE4 revealed normal boundaries of expression in the *Otx2^{FX};Nkx2.1-cre* mutant, despite the lack of invagination of the neural ectoderm (Fig. 5A) (41,46).

Mutants lack FGF10 signaling and have altered cell proliferation

FGF10 positively regulates anterior pituitary gland growth and cell survival (32,46–49). The reduced amount of pituitary tissue in *Otx2^{FX};Nkx2.1cre* mutants could arise from reduced cell proliferation and/or enhanced cell death. Timed pregnant mice were injected with the nucleoside analog, bromo-deoxy uridine (BrdU), and after 2 h, the embryos were collected and processed. Immunohistochemistry for BrdU incorporation during the S-phase of the cell cycle is a proxy for cell proliferation. Normal pituitaries have BrdU immunopositive, proliferating cells all along the ventral diencephalon at e10.5 and e12.5 (marked with white bars), except for the invaginated region

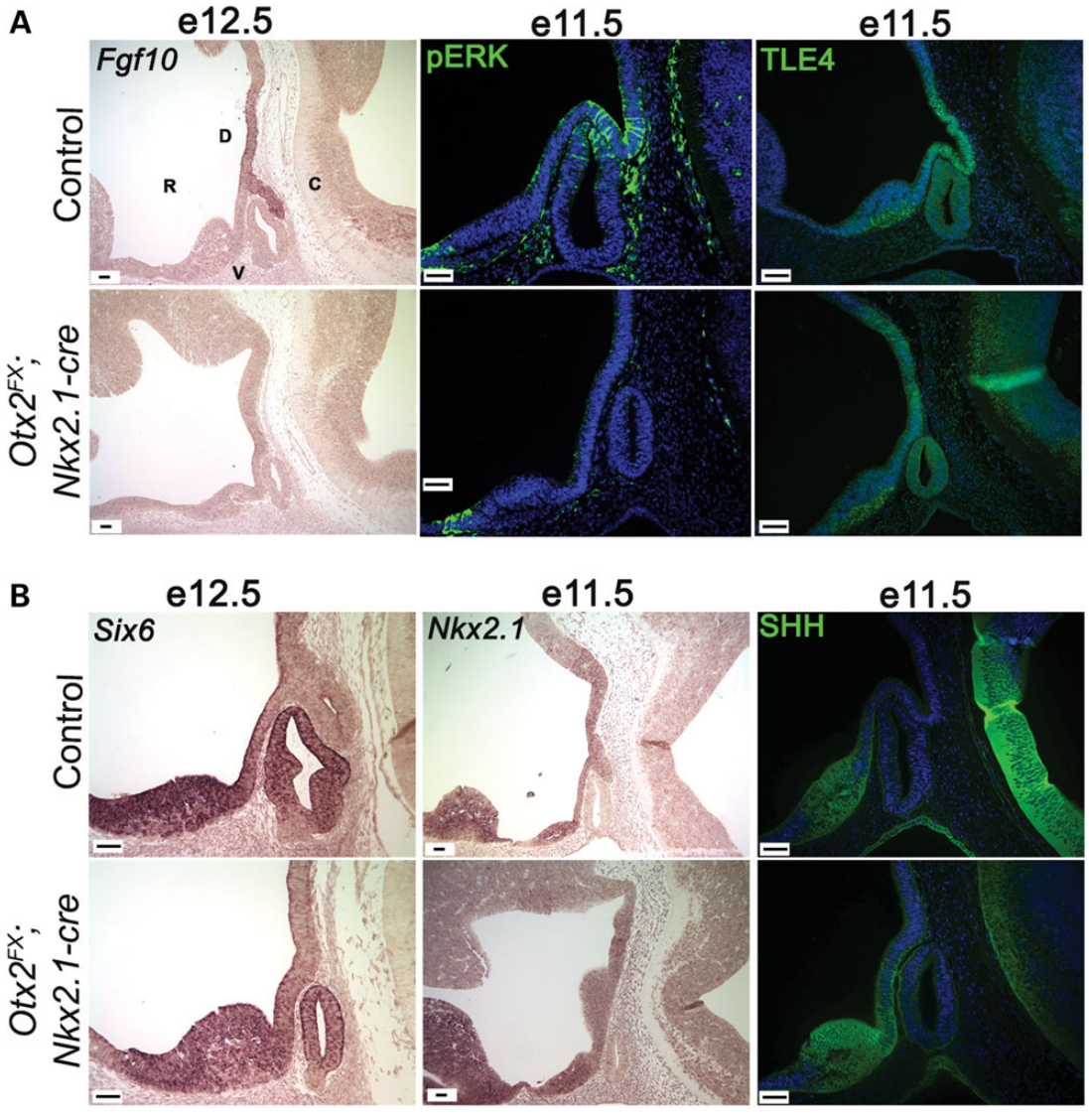

Figure 5. (**A** and **B**) Loss of OTX2 in the ventral diencephalon disrupts FGF signaling. (A) *In situ* hybridization at e12.5 on sagittal sections shows that *Fgf10* is greatly decreased in the ventral diencephalon of *Otx2^{FX};Nkx2.1-cre* mutants (bottom panel) compared with control (top panel). Immunohistochemistry for pERK expression at e11.5 reveals that pERK signaling is reduced in the *Otx2^{FX};Nkx2.1-cre* mutants (bottom panels) compared with control (top panels). Immunohistochemistry for TLE4 at e11.5 shows a slight decrease in expression in mutants (bottom panels) when compared with control (top panels). The photos in first panel were taken at $\times$100. Scale bar: 100 μm. The photos in the middle and last panels were taken at $\times$200. Scale bar: 50 μm. (B) *In situ* hybridization for *Six6* at e12.5 and *Nkx2.1* at e11.5 revealed no difference between mutant (bottom panels) and control pituitaries (top panels). Immunohistochemistry for SHH at e11.5 suggests there is no difference in expression between mutant (bottom panel) and control (top panel) pituitaries. The photos in the first and last panels were taken at. Scale bar: 50 μm. The photos in the middle panel were taken at. Scale bar: 100 μm. D—dorsal, C—caudal, V—ventral, R—rostral.

that will become the infundibulum (Fig. 6A) (49). BrdU immunopositive, proliferating cells are normally present throughout Rathke's pouch, except for the most ventral area where cells are beginning to differentiate at e12.5. At e12.5, the BrdU-labeled cells in *Otx2^{FX};Nkx2.1-cre* mutant pituitaries exhibit an abnormal pattern in the ventral diencephalon, specifically. There are no BrdU-negative cells in *Otx2^{FX};Nkx2.1-cre* mutants at the site where invagination of the ventral diencephalon normally occurs, which is outlined in white (Fig. 6A). At e12.5, the *Otx2^{FX};Nkx2.1-cre* mutant pituitaries have a patch of BrdU-negative cells in the ventral aspect of Rathke's pouch, similar to the pattern in normal mice.

In order to quantify cell proliferation, we calculated the percent of DAPI-stained nuclei that were positive for BrdU immunostaining in specific regions of the pituitary at e10.5 and e12.5 in *Otx2^{FX};Nkx2.1-cre* mutants and controls. At e10.5, there is no significant difference in the average percentage of proliferating cells in the ventral diencephalon (Fig. 6A and B). At e12.5, however, the *Otx2^{FX};Nkx2.1-cre* mutant ventral dienephalon displays a significant increase in the number of proliferating cells (Fig. 6B). The percentage of BrdU-positive cells in Rathke's pouch is significantly decreased at e12.5 in the *Otx2^{FX};Nkx2.1-cre* mutants relative to controls (Fig. 6B). The TUNEL assay was performed at e10.5, e12.5 and e14.5, and no

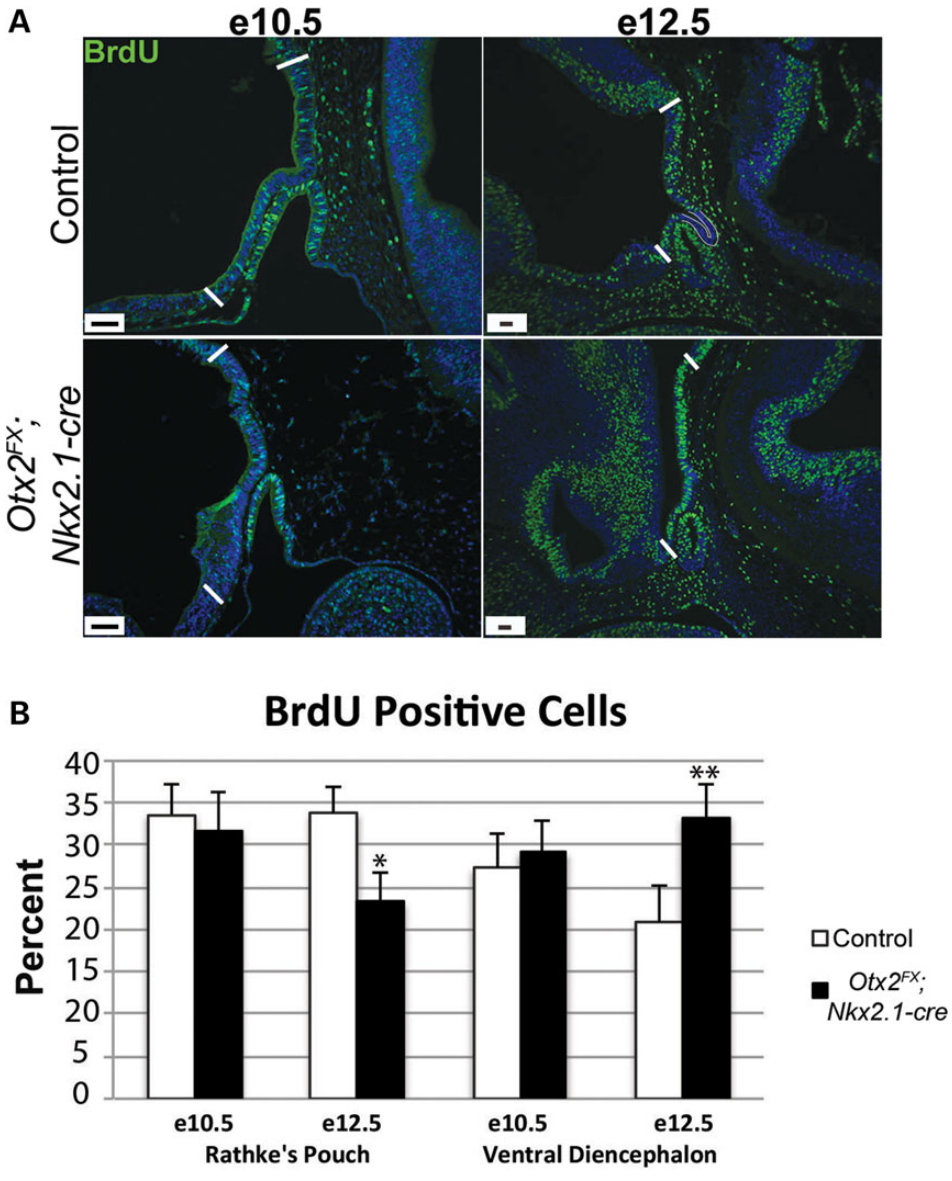

Figure 6. (**A** and **B**) Cell proliferation is affected in the *Otx2^{FX};Nkx2.1-cre* mutant pituitaries. Timed pregnant female mice were injected with BrdU, and embryos were collected after 2 h. (A) Immunohistochemistry was used at e10.5 and e12.5 to detect BrdU-labeled cells. Three controls and three *Otx2^{FX};Nkx2.1-cre* mutants were used for both e10.5 and e12.5. BrdU-labeled cells were counted in Rathke's pouch and in the white marked region of the ventral diencephalon at both e10.5 and e12.5. The region outlined in white in the top right panel is the evaginating ventral diencephalon that will become the posterior lobe in the control pituitary. The photos in the right panel were taken at. Scale bar: 50 μm. The photos in the left panel were taken at. Scale bar: 100 μm. (B) ImageJ IJ 1.46r software with the Cell Counter plug-in from the NIH was used to count the total number of proliferating cells and the Student's *T*-Test was used to determine significance. There is a significant decrease in proliferating cells in Rathke's pouch at e12.5 in the *Otx2^{FX};Nkx2.1-cre* mutants compared with controls ($^{*}P$-value < 0.05) and a significant increase in proliferating cells in the ventral diencephalon at e12.5 in the *Otx2^{FX};Nkx2.1-cre* mutant compared with control ($^{**}P$-value <0.01). There was no significant difference in proliferating cells at e10.5 in either Rathke's pouch or the ventral diencephalon.

differences in cell death were observed in either the ventral diencephalon or Rathke's pouch of *Otx2^{FX};Nkx2.1-cre* mutants (Supplementary Material, Fig. S2).

Loss of OTX2 in the ventral diencephalon does not affect cell specification or hypothalamic–pituitary axis function

To test whether the pituitary cells in *Otx2^{FX};Nkx2.1-cre* mutants were correctly specified, immunohistochemistry was performed at P10 for the hormones TSHβ, ACTH, LHβ, GH, αMSH (Fig. 7A) and FSHβ (data not shown). Immunostaining indicated that all cell types are present, and other than the smaller posterior and anterior lobes in the mutants, there were no obvious differences between the controls and the *Otx2^{FX};Nkx2.1-cre* mutants ($n = 3$). At e14.5, the anterior lobe of the *Otx2^{FX};Nkx2.1-cre* mutants exhibit normal immunostaining for POU1F1 and αGSU (Supplementary Material, Fig. S3). Immunostaining for arginine vasopressin (AVP), a neurohypophysial hormone,

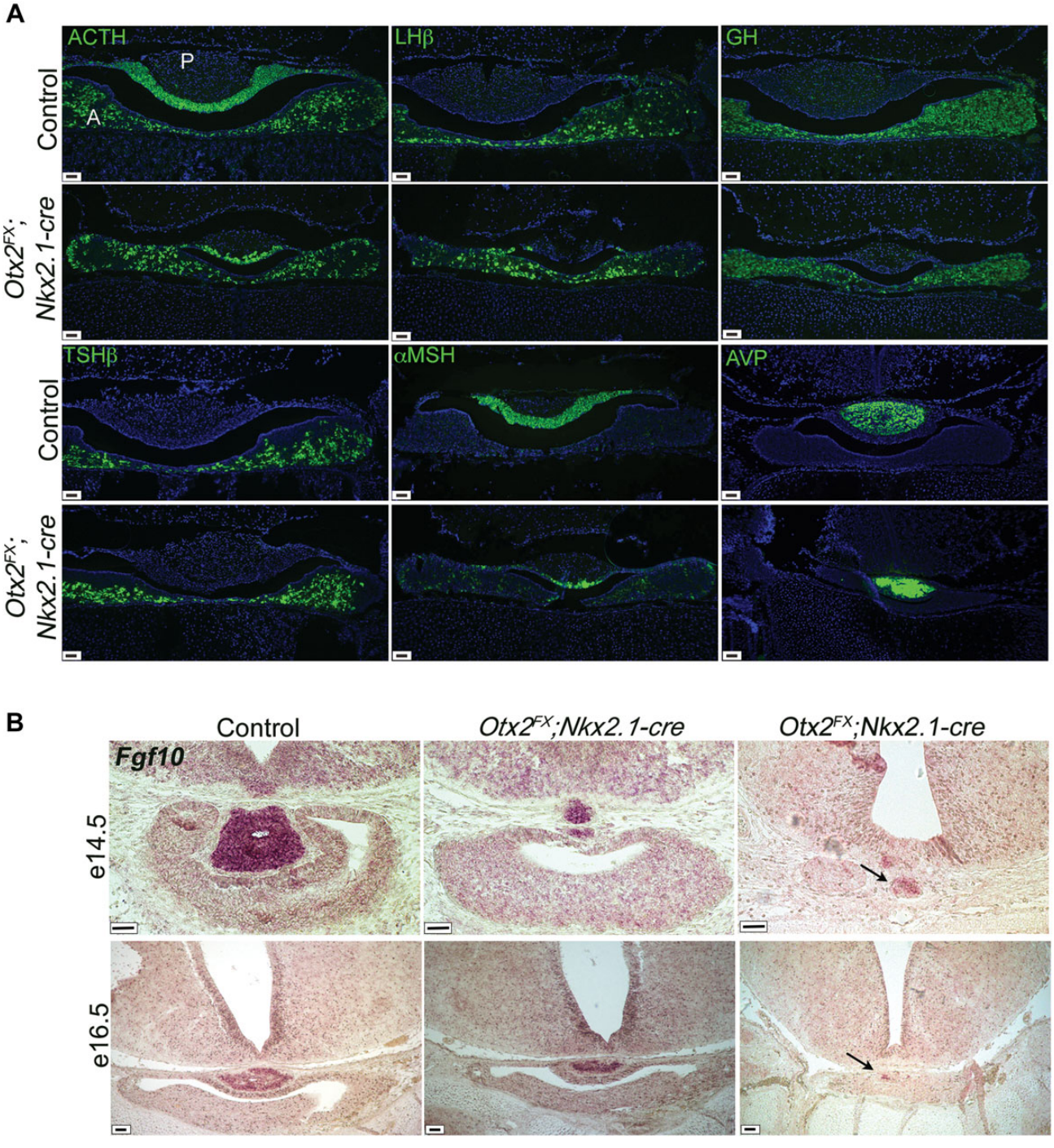

Figure 7. (A) Loss of OTX2 in the ventral diencephalon does not affect cell specification in the anterior pituitary lobe. Immunohistochemistry at P10 on coronal sections for the hormones TSHβ, ACTH, LHβ and GH demonstrate no difference between control and the *Otx2^{FX};Nkx2.1-cre* mutants. Immunohistochemistry on coronal sections at P2 for AVP expression in the posterior lobe reveals no difference between control and the *Otx2^{FX};Nkx2.1-cre* mutants. All photos were taken at ×100. Scale bar: 100 μm. (B) The recovering, mutant infundibulum expresses *Fgf10. In situ* hybridization at e14.5 and e16.5 using coronal sections shows *Fg10* expression in the control infundibulum (left panel). Variable expression on *Fgf10* is also detected in the small infundibulum tissue of the *Otx2^{FX};Nkx.1-cre* mutants at e14.5 and e16.5 (arrows, middle and right panels). The photos in the top panel were taken at. Scale bar: 50 μm. The photos in the bottom panel were taken at. Scale bar: 100 μm.

indicates normal projection of AVP neurons from the hypothalamus to the posterior lobe of the pituitary at P2 in the *Otx2^{FX};Nkx2.1-cre* mutants and controls (Fig. 7A).

We hypothesized that pituitary glands of the *Otx2^{FX};Nkx2.1-cre* mutants were recovering their growth by a resurgence of FGF signaling. Because *Fgf10* expression is no

longer detectable in the posterior lobe at birth (data not shown), we examined expression between e14.5 and e16.5 by *in situ* hybridization in coronal pituitary sections of $Otx2^{FX}$;*Nkx2.1-cre* and control mice. We detected robust *Fgf10* expression in the posterior lobe of control mice at these times. Variable amounts of *Fgf10* expression are detectable in the small, preliminary nubbins of posterior lobe in the $Otx2^{FX}$;*Nkx2.1-cre* mutants (Fig. 7B).

Homozygous mutant mice are viable and present in expected Mendelian ratios ($N = 43$, $P > 0.25$). Surprisingly, there is no obvious difference in growth rate or final adult size of mice at 12 weeks of age. We conducted a fertility study by mating $Otx2^{FX}$;*Nkx2.1-cre* mutant females and males to normal $Otx2^{FX/FX}$ or C57BL/6 mice of the opposite sex. We mated three different $Otx2^{FX}$;*Nkx2.1-cre* mutant and three different $Otx2^{FX/FX}$ control 6-week-old females to three different C57BL/6 adult males in separate cages. All females gave birth to a litter of pups within 5 weeks. All pups survived to weaning age (21 days). We mated three different $Otx2^{FX}$;*Nkx2.1-cre* mutant and three different $Otx2^{FX/FX}$ control 12-week-old males to C57BL/6 females. All females of these matings produced a litter of healthy pups within 6 weeks. This indicates that the hypothalamic–pituitary axes recovered sufficiently to support normal growth and fertility despite the loss of OTX2 protein in the ventral diencephalon.

DISCUSSION

Patients heterozygous for mutations in OTX2 can exhibit varying degrees of pituitary hypoplasia, ectopic posterior pituitary gland, invisible pituitary stalk, CPHD and IGHD. Similarly, mice heterozygous for OTX2 loss of function can have pituitary hypoplasia, missing or misplaced pituitary glands, and/or pituitary dysmorphology (12,50). The pattern of OTX2 expression in the developing mouse pituitary points to a primary role in the development of the pituitary stalk and posterior lobe. OTX2 is expressed strongly in the developing posterior pituitary lobe, hypothalamus and other specific regions of the brain, but expression is modest and transient in Rathke's pouch. To identify the mechanism of OTX2 action in pituitary development, we used a cre-loxP strategy to selectively delete *Otx2* from either the ventral diencephalon, which forms the posterior pituitary lobe, or early head development and Rathke's pouch. We report that disruption of OTX2 in early head development causes a variable dysmorphic pituitary gland phenotype, whereas loss of OTX2 in Rathke's pouch has no effect on cell specification. OTX2 deficiency in the ventral diencephalon has a profound effect on the initial development of the posterior lobe and pituitary stalk. This is associated with reduced and delayed FGF signaling, which secondarily causes anterior lobe hypoplasia. We discovered that FGF signaling becomes active later in gestation, and this may contribute to the recovery of anterior pituitary gland growth in mice with a neural-ectoderm-specific OTX2 disruption. Thus, loss of OTX2 in the neural ectoderm is sufficient to cause severe, but transient, hypopituitarism.

The hormone deficiency and pituitary hypoplasia characteristic of some human patients has been proposed to arise from the inability of the mutant OTX2 to activate HESX1 and POU1F1 appropriately (3–5). In the developing mouse pituitary, however, OTX2 protein is only transiently expressed in Rathke's pouch at e10.5, and it is essentially absent from the anterior lobe when POU1F1 is first detectable (25). As OTX2 and POU1F1 are not expressed in the same cells at the same time, it is not plausible that the patient's hormone deficiency is due to failed activation of Pou1f1. In addition, the *cre* drivers that we used to disrupt *Otx2* in the oral or visceral ectoderm had no effect on *Pou1f1* expression. *Otx2* and *Hesx1* both are expressed in the AVE and later in the anterior neural ectoderm. In fact, previous experiments with $Otx2^{-/-}$ chimeras have shown that *Otx2* is required for the initiation of *Hesx1* transcription during early forebrain development (51). Temporally regulated deletion of *Otx2* during development revealed that this transcription factor has an essential role in head development before e10.5, whereas deletion between e12.5 and e14.5 was compatible with normal morphology but impaired growth, and deletion after e14.5 had no effect on growth (38). Therefore, hypopituitarism most likely originates from early patterning defects during gastrulation (11,19,21,22,52).

We employed several *cre* drivers to assess the significance of the early, transient expression of *Otx2* in Rathke's pouch. Removing OTX2 from Rathke's pouch with either *Prop1-cre* (data not shown) or *Pitx2-cre* did not result in any abnormalities, suggesting that OTX2 does not play a direct or intrinsic role in anterior pituitary development. Because *Pitx2-cre* activity is not 100% penetrant in the cells of Rathke's pouch, it is difficult to rule out the possibility that some transient expression of *Otx2* occurred. *Foxg1-cre* activity is reported to be pituitary specific on certain genetic backgrounds and to label essentially every cell in Rathke's pouch (33,34). OTX2 deletion with *Foxg1-cre* resulted in serious craniofacial defects including anophthalmia, indicating that in this context *Foxg1-cre* caused *Otx2* deficiency in early head development, in addition to the disruption in Rathke's pouch. These fetuses have pituitary dysmorphology but normal cell specification in the anterior lobe. Taken together, the results of these three *cre* driver experiments support the interpretation that pituitary dysmorphology is secondary to a defect in early head development, rather than a result of OTX2 deficiency in Rathke's pouch.

OTX2 is expressed strongly in the region of the ventral diencephalon that forms the posterior lobe, and this region normally has reduced cell proliferation relative to the areas directly above and below it (25). Disruption of OTX2 in this region profoundly affected posterior lobe development. The cells normally fated to become the posterior lobe failed to leave the cell cycle, evaginate, differentiate or produce FGF10. The anterior lobes of these fetuses exhibited reduced cell proliferation and hypoplasia during early development, despite intact *Otx2* expression in Rathke's pouch. This secondary effect is likely due to the lack of FGF signaling from the ventral diencephalon, because disruption of *Fgf* or *Fgfr2* also causes anterior lobe hypoplasia (32,53). We did not observe enhanced cell death in the pituitaries of $Otx2^{FX}$;*Nkx2.1-cre* mutants. This contrasts with the occurrence of increased apoptosis in other neural-derived structures of *Otx2* deficient mice, including the retinal pigment epithelium, photoreceptors, GnRH neurons and the choroid plexus (54–56). This also differs with the $Fgf10^{-/-}$ embryos, which exhibit an agenic pituitary by e15.5 after widespread apoptosis (32). Our mouse model has only a decrease in *Fgf10*, opposed to a complete loss of *Fgf10* throughout the mouse. There are many

reports of OTX2 expression affecting FGF signaling, and vice versa. The effects can be positive or negative (57–60). Thus, the relationship between *Otx2* and FGF signaling may differ among affected organ systems.

There are many factors besides OTX2 that affect development of the posterior lobe, including LHX2, NKX2.1, RAX, HES1, TCF7L2, SOX3, WNT5A, SHH and TBX3 (61). In humans, TBX3 mutations cause a multiple congenital anomaly known as mammary ulnar syndrome, affecting posterior limbs, mammary and apocrine glands, teeth, puberty and genital development (62–64). In mice, the pattern of *Tbx3* expression appears to coincide with *Otx2* in the ventral diencephalon, and there is a trace of *Tbx3* expression in the ventral aspect of Rathke's pouch. Some effects of *Tbx3* deficiency on pituitary development are similar to those we observed in $Otx2^{FX}$;*Nkx2.1-cre* mutants, but the mechanisms appear to be different. *Tbx3* knockout mice fail to generate a region of the ventral diencephalon that is negative for SHH, the cells continue to proliferate, fail to invaginate, and there is a modest, transient change in *Fgf10* expression. Rathke's pouch is significantly smaller, cell proliferation in the anterior lobe is significantly reduced and expression of the signature transcription factors POU1F1 and TPIT are lost. In contrast, the growth defects of $Otx2^{FX}$;*Nkx2.1-cre* mutant pituitaries are associated with intact SHH patterning and near absence of *Fgf10* expression at the normal time of onset. The *Tbx3*-mutant mice die owing to cardiovascular defects after e14.5, so the recovery of infundibular and anterior pituitary growth cannot be investigated in these mice. Nevertheless, the different mechanisms underlying hypoplasia of the posterior lobe and pituitary stalk support the idea that TBX3 and OTX2 act in separate pathways that contribute to normal development of these structures.

The postnatal recovery of growth and function in both the posterior and anterior lobes of $Otx2^{FX}$;*Nkx2.1cre* mutants is surprising, and it suggests the possibility of compensation for *Otx2* deficiency by other genes. FGF signaling may contribute to the recovery because, despite the complete absence of *Fgf10* expression and pERK signaling in mutants at e11.5, *Fgf10* expression is detectable later in gestation. We also considered the possibility that genes related to *Otx2*, such as *Otx1*, are involved in the recovery process. Both the *Otx1* and *Otx2* genes encode bicoid-like homeodomain proteins that share extensive sequence similarities and have functional overlap in some tissues (21,65).

There are several pieces of evidence that argue against the involvement of *Otx1* in the recovery. First, replacement of the *Otx2*-coding sequences with those of *Otx1* does not rescue anterior structures including the eyes, olfactory bulbs, forebrain and pituitary gland (65,66). Second, *Otx1* expression in the anterior lobe is initiated postnatally, after recovery has already begun in the $Otx2^{FX}$, *Nkx2.1-cre* mutants (21,65), and we detected no *Otx1* expression in the infundibulum or Rathke's pouch during early pituitary development (data not shown). Third, there is no increase in *Otx1* transcripts in pituitary glands of $Otx2^{FX}$; *Nkx2.1-cre* mutant mice after birth (data not shown). Thus, OTX1 is less likely to be involved in the recovery than FGF10. The two homeobox genes *Emx1* and *Emx2* also share regions of *Otx2* expression in the forebrain at e10.5 (20). Furthermore, *Emx2* and *Otx2* interact with each in a dose-dependent manner in diencephalon development (67). It is possible that *Emx1* and *Emx2* could compensate for the loss of *Otx2*. There is no increase of *Emx1* and *Emx2* transcripts in the $Otx2^{FX}$;*Nkx2.1-cre* mutant pituitaries (data not shown), but we cannot rule out an increase in neural tissues.

There are at least two loci in mice that suppress or enhance the effects of *Otx2* deficiency (13), although the underlying genes are not yet known. Disruption of *Otx2* in the neural ectoderm might result in a more dramatic phenotype on another genetic background. We analyzed the $Otx2^{FX}$; *Nkx2.1-cre* knockout on a mixed C57BL/6, 129/SvJ background, and while the phenotype was consistent among individuals, it may have been more severe on a pure C57BL/6 genetic background. It is possible that the genes that can suppress the effects of *Otx2* deficiency are contributing to the recovery of pituitary growth in the $Otx2^{FX}$;*Nkx2.1-cre* mice postnatally. There may be regions of early OTX2 expression in the neuroectoderm that do not share expression with NKX2.1 and remain intact in our mouse model. We cannot rule out a contribution of residual OTX2 to the recovery of pituitary growth.

Our results suggest mechanisms that underlie hypopituitarism in patients with *OTX2* mutations. Although OTX2 deficiency in the ventral diencephalon has no effect on *Pou1f1* expression and cell specification or hormone expression, reduction of OTX2 in the neural ectoderm could result in a thin or absent stalk, impairing signaling between the hypothalamus and the pituitary gland. This developmental defect could be persistent if the recovery process is less robust in human pituitary development. The variable ocular, craniofacial and pituitary defects that arose in $Otx2^{FX}$;*Foxg1-cre* mutants are consistent with dosage sensitivity for OTX2 in early head development. An element of chance (stochastic effects) and/or environmental influences (epigenetic effects) could contribute to the variable phenotypes and incomplete penetrance in humans and mice. It is clear, however, that variations in interacting genes that confer enhancing and suppressing effects are important factors (5,10,68). Exome sequencing might identify rare, deleterious variants in genes that enhance the effects of *OTX2* mutations and give further insight into the origin of hypopituitarism.

METHODS AND MATERIALS

Mice

All mice were housed in a 12-h light, 12-h dark cycle in ventilated cages with unlimited access to tap water and Purina 5020 chow. All procedures were conducted in accordance with the principles and procedures outlined in the National Institutes of Health Guidelines of the Care and Use of Experimental Animals. $Otx2^{FX/+}$ mice were provided by Dr Thomas Lamonerie (Institute of Biology Valrose Université Nice, Lyon Gerland, France). The mice were mated to produce homozygotes ($Otx2^{FX/FX}$) and maintained with homozygous matings on the 129/Sv background. The *C57BL/6J-Tg(Nkx2-1-cre)2Sand/J* ($Nkx2.1\text{-}cre^{+/-}$) mice were purchased from The Jackson Laboratory (stock number 008661, Bar Harbour, ME, USA) and maintained by mating to C57BL/6J mice from The Jackson Laboratory. The B6.129S4-*Gt(ROSA)26Sor*^{tm1Sor}/J mice ($R26R^{FX/FX}$) were purchased from The Jackson Laboratory (stock number 003474) and maintained as homozygotes. $Otx2^{FX/FX}$ mice were mated to $Nkx2.1\text{-}cre^{+/-}$ mice to generate $Otx2^{FX/+}$;$Nkx2.1\text{-}cre^{+/-}$ mice. $Otx2^{FX/FX}$ mice were mated to the $R26R^{FX/FX}$

reporter mouse to generate *Otx2*$^{FX/FX}$;*R26R*$^{FX/FX}$ mice. These mice were mated to *Otx2*$^{FX/+}$;*Nkx2.1-cre*$^{+/-}$ mice to generate *Otx2*$^{FX/FX}$;*Nkx2.1-cre*$^{+/-}$; *R26R*$^{FX/+}$mice. The *Pitx2*$^{tm4(cre)Jfm}$ (*Pitx2-cre*) mice were obtained from Dr James F. Martin (University of Texas, Southwestern, Dallas, TX, USA) and maintained by mating to C57BL/6J wild-type mice from Jackson Laboratory. *Otx2*$^{FX/FX}$ mice were mated to *Pitx2-cre*$^{+/-}$ mice to generate *Otx2*$^{FX/+}$;*Pitx2-cre*$^{+/-}$ mice. *Otx2*$^{FX/FX}$;*R26R*$^{FX/FX}$ mice were mated to *Otx2*$^{FX/+}$;*Pitx2-cre*$^{+/-}$ mice to generate *Otx2*$^{FX/FX}$;*Pitx2-cre*$^{+/-}$;*R26R*$^{FX/+}$mice. The *Foxg1*$^{tm1(cre)Skm}$ (*Foxg1-cre*) mice were obtained from Dr Susan K. McConnell (Stanford University, Stanford, CA, USA) and maintained by mating to wild-type Swiss Webster (CFW) mice from Charles River. *Otx2*$^{FX/FX}$ mice were mated to *Foxg1-cre*$^{+/-}$ mice to generate *Otx2*$^{FX/+}$;*Foxg1-cre*$^{+/-}$ mice. *Otx2*$^{FX/FX}$ mice were mated to *Otx2*$^{FX/+}$;*Foxg1-cre*$^{+/-}$ mice to generate *Otx2*$^{FX/FX}$;*Foxg1-cre*$^{+/-}$ mice.

Genotyping was carried out by PCR amplification of genomic DNA as previously described. *Cre*-specific primers were 5′ GCATAACCAGTGAAACAGCATTGCTG 3′ and 5′ GGACA TGTTCAGGGATCGCCAGGCG 3′ (69); *R26R*^{FX} primers were 5′ GGCTTAAAGGCTAACCTGATGTG 3′, 5′ -GCGAA GAGTTTGTCCTCAACC 3′ and 5′ GGAGCGGGAGAAATG GATATG 3′ (69); and *Otx2*^{FX} were primers were 5′ GAACA AACGTCCCTGTGGTG 3′ and 5′ GAGCTTCCAGAACGTC GAG 3′ (38). PCR products were visualized with ethidium bromide on a 1.5–2% agarose gel.

Timed pregnancies were produced using natural matings of sexually mature females and males. The morning after conception is designated e0.5, and the day of birth is designated as P1. This method was used to collect embryos at the times of e10.5, e11.5, e12.5, e14.5 and e16.5 and postnatal mice at P2 and P10.

Tissue preparation and histology

Embryos were fixed in 4% formaldehyde in PBS at 4°C for 30 min for e10.5 and e11.5 embryos, for 1 h for e12.5 embryos, for 2 h for e14.5 and e16.5 embryos, and overnight for P2 and P10 mice. The tissue was washed with PBS, dehydrated to 70% ethanol and embedded in a Tissue Tek VIP Paraffin tissue processing machine (Miles Scientific). Six-micrometer-thick sagittal sections were prepared from embryos collected at e10.5 through e16.5, and coronal sections were prepared from some e14.5 embryos and postnatal pups. For hematoxylin and eosin (Sigma–Aldrich) staining, the paraffin-embedded tissue sections were soaked in xylene to remove the paraffin and hydrated by soaking slides in 100% ethanol, 95% ethanol and finally distilled water. The slides were next soaked in hematoxylin for 30 s, rinsed in distilled water, soaked in eosin for 20 s and then rinsed in distilled water. The slides were dehydrated back to xylene and mounted with xylene/permount 1 : 2 (Fisher) mounting media. For frozen sections, tissue was fixed in 4% paraformaldehyde in PBS at 4°C for the times previously described, rinsed in PBS and soaked in 30% sucrose at 4° C until the tissue sank to the bottom of the container. This fixed tissue was embedded in OCT (Tissue-Tek), frozen on dry ice and placed at −80°C prior to sectioning at a thickness of 16 μm. X-gal staining and neutral red staining were performed as previously described (69,70).

Immunohistochemistry and *in situ* hybridization

Immunostaining for pituitary hormone markers was performed using anti-TSHβ, ACTH, LHβ, FSHβ, GH (1 : 1000, National Hormone and Peptide Program, UCLA Medical Center, Torrance, CA, USA), and anti-α-MSH (AB5087, 1 : 100, Chemicon, Temecula, CA, USA) antibodies, on paraffin sections. Sections were hydrated, incubated for 20 min in 3% H_2O_2 : 50% methanol to block endogenous peroxidases. All slides were placed in normal goat serum block (5% goat serum, 3% BSA and 0.5% Tween-20 in PBS) for 10 min at room temperature. All hormone antibodies were diluted in blocking solution and incubated on the slides overnight at 4°C, except for GH, which was incubated for 1 h at room temperature. When staining for anti-OTX2 (ab21990, 1 : 1000, Abcam, Cambridge, MA, USA), anti-TLE4 (1 : 1000, from Dr Stefano Stefani), anti-pERK (1 : 100, 4370, Cell Signaling), anti-AVP (1 : 500, ab39363, Abcam), SHH (AF464, 1 : 200, R&D Systems), anti-PITX1 (1 : 100, from Dr Jacques Drouin) and anti-TPIT (1 : 200, from Dr Jacques Drouin), paraffin sections were first boiled in 0.01 M citrate for 10 min, followed by 20 min of incubation in 3% H_2O_2 : 50% methanol, and were incubated for 10 min in normal goat serum block, except for SHH slides, which required a 5% normal donkey serum block. Antibodies were incubated overnight at 4°C. The following secondary antibodies were used: biotinylated anti-rabbit IgG (BA-1000, 1 : 200, Vector Laboratories, Burlingame, CA, USA) for anti-TSHβ, ACTH, FSHβ OTX2, TLE4, pERK and AVP; anti-human biotin (1 : 200, ab97223, Abcam) for anti-GH, biotinylated anti-guinea pig IgG for anti-LHβ, biotin-conjugated anti-goat IgG (1 : 200, 305-066-047, Jackson Immunoresearch) for anti-SHH and biotin anti-sheep IgG (1 : 200, 313-065-047, Jackson Immunoresearch) for anti-αMSH. Antibodies were detected using either the tyramide signal amplification (TSA) and fluorescein isothiocynate kit (according to protocol, Perkin–Elmer, Boston, MA, USA) or streptavidin-conjugated Alexa-fluor 488 (1 : 200, S11223, Invitrogen). Cell proliferation detection was performed as described by (71) and using 100 mg BrdU per gram of body weight injected into pregnant mice by intraperitoneal injection 2 h prior to collecting embryos. After processing, tissue sections were boiled in 0.01 M citrate for 10 min, followed by 20 min of incubation in 3% H_2O_2 : 50% methanol and incubated for 1 h in a mouse IgG block. The secondary biotin anti-rat IgG (1 : 200, 711-066-152, Jackson Immunoresearch, Westgrove, PA, USA), and the TSA kit were used for detection. Cell nuclei were stained with DAPI (1 : 200) for 5 min. Slides were mounted with permount mounting medium.

Cell death was detected using the *In Situ* Cell Death Detection Kit, Fluorescein (Roche), which labels DNA strand breaks with TUNEL technology. Paraffin sections were rehydrated as described earlier and then permealibilzed with 20 μg/ml Proteinase K in 10 mM Tris–HCL, pH 8. The TUNEL labeling was carried out according to the published protocol, and the cell nuclei were stained with DAPI (1 : 200) for 5 min. Cell nuclei were stained with DAPI (1 : 200) for 5 min. Slides were mounted with permount mounting medium.

In situ hybridization

Lori Sussel (Columbia University, NY) provided a mouse *Nkx2.1* clone in a pSK+ plasmid. The sequence was linearized with *SalI* and labeled with T3 polymerase. Bridget Hogan

(Duke University) provided a mouse *Fgf10* clone in a pKSII+ plasmid. The sequence was linearized with BamHI and labeled with T3 polymerase. The mouse *Six6* clone in a pFLCI plasmid was linearized with BamHI and labeled with T7 polymerase. Juan Pedro Martinez-Barbera (University College London, UK) provided a mouse *Otx1* clone. The sequence was linearized with EcoR1 and labeled with Sp6. Paul Thomas (University of Adelaide, Australia) provided the mouse *Hesx1* clone. The sequence was linearized with BamHI and labeled with T3 polymerase. The probes were diluted 1 : 100 and hybridized at 55°C. The mouse *Otx2* clone in a pFLCI plasmid was linearized with SmaI and and labeled with T7 polymerase. The *Otx2 in situ* probe was diluted 1 : 200 and hybridized at 60°C. All riboprobes were generated and labeled with digoxigenin and precipitated with nitro-blue tetrazolium chloride/5-bromo-4-chloro-3-indolyl phosphate (Roche Molecular Biochemicals, Indianapolis, IN, USA) using previously described methods (72,73). All images were taken with a Leica Leitz DMB microscope and Leica DFC310 FX camera. Images were analyzed with Leica Application Suite Software V2.7 and Adobe Photoshop CS6 V13.0.

Isolation of RNA from pituitaries

Postnatal day 1 pituitaries were collected and stored in RNAlater (Ambion, Austin, TX, USA) at (−20°C). RNAlater was removed, and pituitaries were placed in 300 μl lysis buffer from the RNAqueous 4PCR Kit (AMbion). Pituitaries were homogenized using an Ultra-Turrax T8 homogenizer (IKA, Wilmington, NC, USA). Total RNA was isolated with RNAqueous Micro Kit according to manufacturer's instructions. RNA quantity (determined by A260 value) and quality (determined by A260/A280 ratio) were analyzed with a NanoDropTM 1000 Spectrophotometer (Thermo Scientific, Waltham, MA, USA).

RT-qPCR

Synthesis of cDNA was carried out as described (74). The following primers were designed to amplify *Otx1* cDNA across exons 2 and 3: 5′ GCAAAGACTCGCTACCCAGA 3′; 5′ G GTTTTCGTTCCATTCCCGC 3′. The following primers were designed to amplify *Emx1* cDNA across exons 2 and 3: 5′ G CGAGCCTTTGAGAAGAATCAC 3′; 5′ CCGATTCTGGAA CCACACCTT 3′. The following primers were designed to amplify *Emx2* cDNA across exons 2 and 3: 5′ AACCATTAC GTGGTGGGAGC 3′; 5′ CGCCTGCTTGGTAGCAATTC 3′. PCR products were visualized with ethidium bromide on a 1.5% agarose gel, and bands were confirmed as *Otx1, Emx1* and *Emx2* PCR products through standard Sanger sequencing at the University of Michigan Sequencing Core. PCR amplification of the housekeeping gene *Hprt* served as an internal control for each RNA sample.

Pituitary area

Hematoxylin and Eosin Staining (H&E) was performed at P2. Three wild-types and three mutants were analyzed. Four sections were selected at five section intervals from each sample. ImageJ IJ 1.46r software from The National Institute of Health (NIH) was used to measure the posterior and anterior lobes with the trace tool. Images were converted from pixels to centimeters. Average area was calculated for anterior and posterior lobe, as well as standard of deviations and statistical significance using a Student's T-Test, with Excel Software. The average area and standard deviation was divided by 50 because the original images were taken at × 50 magnification. The area was converted from centimeters to micrometers. Graphs were created with Excel software.

Pituitary size

Relative pituitary size was measured at e14.5, P2 and P10. Sagittal sections were used for e14.5 embryos, and coronal sections were used for P2 and P10 mice. Three controls and three $Otx2^{FX}$;*Nkx2.1-cre* mutants were sectioned with two sections per slide. The number of sections with pituitary gland tissue was counted for each age and genotype. The average number of sections, standard deviations, significance using a Student's T-Test, and graphs were calculated using Excel Software. To calculate percentage, the average number of $Otx2^{FX}$;*Nkx2.1-cre* sections was divided by the average number of control sections for each time point.

BrdU cell proliferation counting

Timed pregnant female mice were injected with BrdU, and after 2 h, embryos were collected. BrdU immunostaining was performed at both e10.5 and e12.5. Images were taken at × 20 magnification for DAPI only, BrdU only and the composite for each embryo. Four wild types and four mutants were analyzed. ImageJ IJ 1.46r software from the NIH was used to calculate the number of proliferating cells (BrdU-labeled cells) compared with the total number of DAPI cells. Cells were counted in the region of the ventral diencephalon (as marked on BrdU figure) as well as in Rathke's pouch. The counting was done by using the Cell Counter plug-in available from the Image J software. The average number of cells, standard deviations, significance using a Student's T-Test and graphs were calculated using Excel Software.

SUPPLEMENTARY MATERIAL

Supplementary Material is available at *HMG* online.

Conflict of Interest statement. None declared.

FUNDING

This work was supported by the National Institute of Heath (grant number R01HD30428 SAC).

REFERENCES

1. Ragge, N.K., Brown, A.G., Poloschek, C.M., Lorenz, B., Henderson, R.A., Clarke, M.P., Russell-Eggitt, I., Fielder, A., Gerrelli, D., Martinez-Barbera, J.P. *et al.* (2005) Heterozygous mutations of OTX2 cause severe ocular malformations. *Am. J. Hum. Genet.*, **76**, 1008–1022.
2. Diaczok, D., Romero, C., Zunich, J., Marshall, I. and Radovick, S. (2008) A novel dominant negative mutation of OTX2 associated with combined pituitary hormone deficiency. *J. Clin. Endocr. Metab.*, **93**, 4351–4359.
3. Dateki, S., Fukami, M., Sato, N., Muroya, K., Adachi, M. and Ogata, T. (2008) OTX2 mutation in a patient with anophthalmia, short stature, and partial GH deficiency: functional studies using the IRBP, HESX1, and POU1F1 promoters. *J. Clin. Endocr. Metab.*, **93**, 3697–3702.
4. Tajima, T., Ohtake, A., Hoshino, M., Amemiya, S., Sasaki, N., Ishizu, K. and Fujieda, K. (2009) OTX2 loss of function mutation causes anophthalmia and combined pituitary hormone deficiency with a small anterior and ectopic posterior pituitary. *J. Clin. Endocr. Metab.*, **94**, 314–319.

5. Dateki, S., Kosaka, K., Hasegawa, K., Tanaka, H., Azuma, N., Yokoya, S., Muroya, K., Adachi, M., Tajima, T., Motomura, K. *et al.* (2010) Heterozygous orthodenticle homeobox 2 mutations are associated with variable pituitary phenotype. *J. Clin. Endocr. Metab.*, **95**, 756–764.
6. Henderson, R.H., Williamson, K.A., Kennedy, J.S., Webster, A.R., Holder, G.E., Robson, A.G., FitzPatrick, D.R., van Heyningen, V. and Moore, A.T. (2009) A rare de novo nonsense mutation in OTX2 causes early onset retinal dystrophy and pituitary dysfunction. *Mol. Vis.*, **15**, 2442–2447.
7. McCabe, M.J., Alatzoglou, K.S. and Dattani, M.T. (2011) Septo-optic dysplasia and other midline defects: the role of transcription factors: HESX1 and beyond. *Best. Pract. Res. Clin. Endocrinol. Metab.*, **25**, 115–124.
8. Wyatt, A., Bakrania, P., Bunyan, D.J., Osborne, R.J., Crolla, J.A., Salt, A., Ayuso, C., Newbury-Ecob, R., Abou-Rayyah, Y., Collin, J.R. *et al.* (2008) Novel heterozygous OTX2 mutations and whole gene deletions in anophthalmia, microphthalmia and coloboma. *Hum. Mutat.*, **29**, E278–E283.
9. Dipple, K.M. and McCabe, E.R. (2000) Modifier genes convert "simple" Mendelian disorders to complex traits. *Mol. Genet. Metab.*, **71**, 43–50.
10. Ashkenazi-Hoffnung, L., Lebenthal, Y., Wyatt, A.W., Ragge, N.K., Dateki, S., Fukami, M., Ogata, T., Phillip, M. and Gat-Yablonski, G. (2010) A novel loss-of-function mutation in OTX2 in a patient with anophthalmia and isolated growth hormone deficiency. *Hum. Genet.*, **127**, 721–729.
11. Acampora, D., Mazan, S., Lallemand, Y., Avantaggiato, V., Maury, M., Simeone, A. and Brulet, P. (1995) Forebrain and midbrain regions are deleted in Otx2-/- mutants due to a defective anterior neuroectoderm specification during gastrulation. *Development*, **121**, 3279–3290.
12. Matsuo, I., Kuratani, S., Kimura, C., Takeda, N. and Aizawa, S. (1995) Mouse Otx2 functions in the formation and patterning of rostral head. *Gene Dev.*, **9**, 2646–2658.
13. Hide, T., Hatakeyama, J., Kimura-Yoshida, C., Tian, E., Takeda, N., Ushio, Y., Shiroishi, T., Aizawa, S. and Matsuo, I. (2002) Genetic modifiers of otocephalic phenotypes in Otx2 heterozygous mutant mice. *Development*, **129**, 4347–4357.
14. Davis, S.W., Potok, M.A., Brinkmeier, M.L., Carninci, P., Lyons, R.H., MacDonald, J.W., Fleming, M.T., Mortensen, A.H., Egashira, N., Ghosh, D. *et al.* (2009) Genetics, gene expression and bioinformatics of the pituitary gland. *Horm. Res.*, **71** Suppl 2, 101–115.
15. Birchmeier, C. and Treier, M. (2001) Genomics boosts mouse molecular genetics. *Trends Genet.*, **17**, 691–692.
16. Treier, M., O'Connell, S., Gleiberman, A., Price, J., Szeto, D.P., Burgess, R., Chuang, P.T., McMahon, A.P. and Rosenfeld, M.G. (2001) Hedgehog signaling is required for pituitary gland development. *Development*, **128**, 377–386.
17. Acampora, D., Di Giovannantonio, L.G. and Simeone, A. (2013) Otx2 is an intrinsic determinant of the embryonic stem cell state and is required for transition to a stable epiblast stem cell condition. *Development*, **140**, 43–55.
18. Ang, S.L., Conlon, R.A., Jin, O. and Rossant, J. (1994) Positive and negative signals from mesoderm regulate the expression of mouse Otx2 in ectoderm explants. *Development*, **120**, 2979–2989.
19. Hermesz, E., Mackem, S. and Mahon, K.A. (1996) Rpx: a novel anterior-restricted homeobox gene progressively activated in the prechordal plate, anterior neural plate and Rathke's pouch of the mouse embryo. *Development*, **122**, 41–52.
20. Simeone, A., Acampora, D., Gulisano, M., Stornaiuolo, A. and Boncinelli, E. (1992) Nested expression domains of four homeobox genes in developing rostral brain. *Nature*, **358**, 687–690.
21. Simeone, A., Acampora, D., Mallamaci, A., Stornaiuolo, A., D'Apice, M.R., Nigro, V. and Boncinelli, E. (1993) A vertebrate gene related to orthodenticle contains a homeodomain of the bicoid class and demarcates anterior neuroectoderm in the gastrulating mouse embryo. *EMBO J.*, **12**, 2735–2747.
22. Thomas, P. and Beddington, R. (1996) Anterior primitive endoderm may be responsible for patterning the anterior neural plate in the mouse embryo. *Curr. Biol.*, **6**, 1487–1496.
23. Dasen, J.S., Barbera, J.P., Herman, T.S., Connell, S.O., Olson, L., Ju, B., Tollkuhn, J., Baek, S.H., Rose, D.W. and Rosenfeld, M.G. (2001) Temporal regulation of a paired-like homeodomain repressor/TLE corepressor complex and a related activator is required for pituitary organogenesis. *Gene Dev.*, **15**, 3193–3207.
24. Dattani, M.T., Martinez-Barbera, J.P., Thomas, P.Q., Brickman, J.M., Gupta, R., Martensson, I.L., Toresson, H., Fox, M., Wales, J.K., Hindmarsh, P.C. *et al.* (1998) Mutations in the homeobox gene HESX1/Hesx1 associated with septo-optic dysplasia in human and mouse. *Nat. Genet.*, **19**, 125–133.
25. Mortensen, A.H., MacDonald, J.W., Ghosh, D. and Camper, S.A. (2011) Candidate genes for panhypopituitarism identified by gene expression profiling. *Physiol. Genomics*, **43**, 1105–1116.
26. Bodner, M., Castrillo, J.L., Theill, L.E., Deerinck, T., Ellisman, M. and Karin, M. (1988) The pituitary-specific transcription factor GHF-1 is a homeobox-containing protein. *Cell*, **55**, 505–518.
27. Camper, S.A., Saunders, T.L., Katz, R.W. and Reeves, R.H. (1990) The Pit-1 transcription factor gene is a candidate for the murine Snell dwarf mutation. *Genomics*, **8**, 586–590.
28. Li, S., Crenshaw, E.B. 3rd, Rawson, E.J., Simmons, D.M., Swanson, L.W. and Rosenfeld, M.G. (1990) Dwarf locus mutants lacking three pituitary cell types result from mutations in the POU-domain gene pit-1. *Nature*, **347**, 528–533.
29. Pfaffle, R.W., Blankenstein, O., Wuller, S. and Kentrup, H. (1999) Combined pituitary hormone deficiency: role of Pit-1 and Prop-1. *Acta Paediatr. Suppl.*, **88**, 33–41.
30. Pfaffle, R.W., Parks, J.S., Brown, M.R. and Heimann, G. (1993) Pit-1 and pituitary function. *J. Pediatr. Endocrinol.*, **6**, 229–233.
31. Kelberman, D., Turton, J.P., Woods, K.S., Mehta, A., Al-Khawari, M., Greening, J., Swift, P.G., Otonkoski, T., Rhodes, S.J. and Dattani, M.T. (2009) Molecular analysis of novel PROP1 mutations associated with combined pituitary hormone deficiency (CPHD). *Clin. Endocrinol.*, **70**, 96–103.
32. Ohuchi, H., Hori, Y., Yamasaki, M., Harada, H., Sekine, K., Kato, S. and Itoh, N. (2000) FGF10 acts as a major ligand for FGF receptor 2 IIIb in mouse multi-organ development. *Biochem. Bioph. Res. Co.*, **277**, 643–649.
33. Hebert, J.M. and McConnell, S.K. (2000) Targeting of cre to the Foxg1 (BF-1) locus mediates loxP recombination in the telencephalon and other developing head structures. *Dev. Biol*, **222**, 296–306.
34. Wang, Y., Martin, J.F. and Bai, C.B. (2010) Direct and indirect requirements of Shh/Gli signaling in early pituitary development. *Dev. Biol.*, **348**, 199–209.
35. Alatzoglou, K.S. and Dattani, M.T. (2012) Phenotype-genotype correlations in congenital isolated growth hormone deficiency (IGHD). *Indian J. Pediatr.*, **79**, 99–106.
36. Beby, F. and Lamonerie, T. (2013) The homeobox gene Otx2 in development and disease. *Exp. Eye Res.*, **111**, 9–16.
37. Liu, W., Selever, J., Lu, M.F. and Martin, J.F. (2003) Genetic dissection of Pitx2 in craniofacial development uncovers new functions in branchial arch morphogenesis, late aspects of tooth morphogenesis and cell migration. *Development*, **130**, 6375–6385.
38. Fossat, N., Chatelain, G., Brun, G. and Lamonerie, T. (2006) Temporal and spatial delineation of mouse Otx2 functions by conditional self-knockout. *EMBO. Rep.*, **7**, 824–830.
39. Soriano, P. (1999) Generalized lacZ expression with the ROSA26 Cre reporter strain. *Nat. Genet.*, **21**, 70–71.
40. Xu, Q., Tam, M. and Anderson, S.A. (2008) Fate mapping Nkx2.1-lineage cells in the mouse telencephalon. *J. Comp. Neurol.*, **506**, 16–29.
41. Brinkmeier, M.L., Potok, M.A., Cha, K.B., Gridley, T., Stifani, S., Meeldijk, J., Clevers, H. and Camper, S.A. (2003) TCF and Groucho-related genes influence pituitary growth and development. *Mol. Endocrinol.*, **17**, 2152–2161.
42. De Moerlooze, L., Spencer-Dene, B., Revest, J.M., Hajihosseini, M., Rosewell, I. and Dickson, C. (2000) An important role for the IIIb isoform of fibroblast growth factor receptor 2 (FGFR2) in mesenchymal-epithelial signalling during mouse organogenesis. *Development*, **127**, 483–492.
43. Davis, S.W. and Camper, S.A. (2007) Noggin regulates Bmp4 activity during pituitary induction. *Dev. Biol.*, **305**, 145–160.
44. Brinkmeier, M.L., Potok, M.A., Davis, S.W. and Camper, S.A. (2007) TCF4 deficiency expands ventral diencephalon signaling and increases induction of pituitary progenitors. *Dev. Biol.*, **311**, 396–407.
45. Potok, M.A., Cha, K.B., Hunt, A., Brinkmeier, M.L., Leitges, M., Kispert, A. and Camper, S.A. (2008) WNT signaling affects gene expression in the ventral diencephalon and pituitary gland growth. *Dev. Dyn.*, **237**, 1006–1020.
46. Takuma, N., Sheng, H.Z., Furuta, Y., Ward, J.M., Sharma, K., Hogan, B.L., Pfaff, S.L., Westphal, H., Kimura, S. and Mahon, K.A. (1998) Formation of Rathke's pouch requires dual induction from the diencephalon. *Development*, **125**, 4835–4840.
47. Ericson, J., Norlin, S., Jessell, T.M. and Edlund, T. (1998) Integrated FGF and BMP signaling controls the progression of progenitor cell differentiation and the emergence of pattern in the embryonic anterior pituitary. *Development*, **125**, 1005–1015.

48. Norlin, S., Nordstrom, U. and Edlund, T. (2000) Fibroblast growth factor signaling is required for the proliferation and patterning of progenitor cells in the developing anterior pituitary. *Mech. Develop.*, **96**, 175–182.
49. Treier, M., Gleiberman, A.S., O'Connell, S.M., Szeto, D.P., McMahon, J.A., McMahon, A.P. and Rosenfeld, M.G. (1998) Multistep signaling requirements for pituitary organogenesis in vivo. *Gene. Dev.*, **12**, 1691–1704.
50. Larder, R., Kimura, I., Meadows, J., Clark, D.D., Mayo, S. and Mellon, P.L. (2013) Gene dosage of Otx2 is important for fertility in male mice. *Mol. Cell. Endocrinol.*, **377**, 16–22.
51. Rhinn, M., Dierich, A., Le Meur, M. and Ang, S. (1999) Cell autonomous and non-cell autonomous functions of Otx2 in patterning the rostral brain. *Development*, **126**, 4295–4304.
52. Simeone, A., Gulisano, M., Acampora, D., Stornaiuolo, A., Rambaldi, M. and Boncinelli, E. (1992) Two vertebrate homeobox genes related to the Drosophila empty spiracles gene are expressed in the embryonic cerebral cortex. *EMBO J.*, **11**, 2541–2550.
53. Hajihosseini, M.K. (2008) Fibroblast growth factor signaling in cranial suture development and pathogenesis. *Front. Oral Biol.*, **12**, 160–177.
54. Beby, F., Housset, M., Fossat, N., Le Greneur, C., Flamant, F., Godement, P. and Lamonerie, T. (2010) Otx2 gene deletion in adult mouse retina induces rapid RPE dystrophy and slow photoreceptor degeneration. *PLoS One*, **5**, e11673.
55. Diaczok, D., Divall, S., Matsuo, I., Wondisford, F.E., Wolfe, A.M. and Radovick, S. (2011) Deletion of otx2 in GnRH neurons results in a mouse model of hypogonadotropic hypogonadism. *Mol. Endocrinol.*, **25**, 833–846.
56. Johansson, P.A., Irmler, M., Acampora, D., Beckers, J., Simeone, A. and Gotz, M. (2013) The transcription factor Otx2 regulates choroid plexus development and function. *Development*, **140**, 1055–1066.
57. Robel, L., Ding, M., James, A.J., Lin, X., Simeone, A., Leckman, J.F. and Vaccarino, F.M. (1995) Fibroblast growth factor 2 increases Otx2 expression in precursor cells from mammalian telencephalon. *J. Neurosci.*, **15**, 7879–7891.
58. Acampora, D., Avantaggiato, V., Tuorto, F. and Simeone, A. (1997) Genetic control of brain morphogenesis through Otx gene dosage requirement. *Development*, **124**, 3639–3650.
59. Broccoli, V., Boncinelli, E. and Wurst, W. (1999) The caudal limit of Otx2 expression positions the isthmic organizer. *Nature*, **401**, 164–168.
60. Greber, B., Coulon, P., Zhang, M., Moritz, S., Frank, S., Muller-Molina, A.J., Arauzo-Bravo, M.J., Han, D.W., Pape, H.C. and Scholer, H.R. (2011) FGF signalling inhibits neural induction in human embryonic stem cells. *EMBO J.*, **30**, 4874–4884.
61. Pearson, C.A. and Placzek, M. (2013) Development of the medial hypothalamus: forming a functional hypothalamic-neurohypophyseal interface. *Curr. Top. Dev. Biol.*, **106**, 49–88.
62. Bamshad, M., Lin, R.C., Law, D.J., Watkins, W.C., Krakowiak, P.A., Moore, M.E., Franceschini, P., Lala, R., Holmes, L.B., Gebuhr, T.C. *et al.* (1997) Mutations in human TBX3 alter limb, apocrine and genital development in ulnar-mammary syndrome. *Nat. Genet.*, **16**, 311–315.
63. Bamshad, M., Root, S. and Carey, J.C. (1996) Clinical analysis of a large kindred with the Pallister ulnar-mammary syndrome. *Am. J. Med Genet.*, **65**, 325–331.
64. Trowe, M.O., Zhao, L., Weiss, A.C., Christoffels, V., Epstein, D.J. and Kispert, A. (2013) Inhibition of Sox2-dependent activation of Shh in the ventral diencephalon by Tbx3 is required for formation of the neurohypophysis. *Development*, **140**, 2299–2309.
65. Acampora, D., Mazan, S., Tuorto, F., Avantaggiato, V., Tremblay, J.J., Lazzaro, D., di Carlo, A., Mariano, A., Macchia, P.E., Corte, G. *et al.* (1998) Transient dwarfism and hypogonadism in mice lacking Otx1 reveal prepubescent stage-specific control of pituitary levels of GH, FSH and LH. *Development*, **125**, 1229–1239.
66. Suda, Y., Nakabayashi, J., Matsuo, I. and Aizawa, S. (1999) Functional equivalency between Otx2 and Otx1 in development of the rostral head. *Development*, **126**, 743–757.
67. Suda, Y., Hossain, Z.M., Kobayashi, C., Hatano, O., Yoshida, M., Matsuo, I. and Aizawa, S. (2001) Emx2 directs the development of diencephalon in cooperation with Otx2. *Development*, **128**, 2433–2450.
68. Schilter, K.F., Schneider, A., Bardakjian, T., Soucy, J.F., Tyler, R.C., Reis, L.M. and Semina, E.V. (2011) OTX2 microphthalmia syndrome: four novel mutations and delineation of a phenotype. *Clin. Genet.*, **79**, 158–168.
69. Charles, M.A., Mortensen, A.H., Potok, M.A. and Camper, S.A. (2008) Pitx2 deletion in pituitary gonadotropes is compatible with gonadal development, puberty, and fertility. *Genesis*, **46**, 507–514.
70. Brinkmeier, M.L., Gordon, D.F., Dowding, J.M., Saunders, T.L., Kendall, S.K., Sarapura, V.D., Wood, W.M., Ridgway, E.C. and Camper, S.A. (1998) Cell-specific expression of the mouse glycoprotein hormone alpha-subunit gene requires multiple interacting DNA elements in transgenic mice and cultured cells. *Mol. Endocrinol.*, **12**, 622–633.
71. Ward, R.D., Raetzman, L.T., Suh, H., Stone, B.M., Nasonkin, I.O. and Camper, S.A. (2005) Role of PROP1 in pituitary gland growth. *Mol. Endocrinol.*, **19**, 698–710.
72. Cushman, L.J., Watkins-Chow, D.E., Brinkmeier, M.L., Raetzman, L.T., Radak, A.L., Lloyd, R.V. and Camper, S.A. (2001) Persistent Prop1 expression delays gonadotrope differentiation and enhances pituitary tumor susceptibility. *Hum. Mol. Genet.*, **10**, 1141–1153.
73. Suh, H., Gage, P.J., Drouin, J. and Camper, S.A. (2002) Pitx2 is required at multiple stages of pituitary organogenesis: pituitary primordium formation and cell specification. *Development*, **129**, 329–337.
74. Vesper, A.H., Raetzman, L.T. and Camper, S.A. (2006) Role of prophet of Pit1 (PROP1) in gonadotrope differentiation and puberty. *Endocrinology*, **147**, 1654–1663.